Hindawi Publishing Corporation
International Journal of Photoenergy
Volume 2014, Article ID 491475, 8 pages
http://dx.doi.org/10.1155/2014/491475

Research Article

Crystalline Silicon Solar Cells with Thin Silicon Passivation Film Deposited prior to Phosphorous Diffusion

Ching-Tao Li,[1] Fangchi Hsieh,[2] Shi Yan,[2] Cuifeng Wan,[2] Yakun Liu,[2] Jing Chen,[2] and Likarn Wang[1]

[1] *Institute of Photonics Technologies, National Tsing Hua University, Hsinchu 30013, Taiwan*
[2] *Jiangsu Aide Solar Energy Technology Co., Ltd., Xuzhou 221121, China*

Correspondence should be addressed to Likarn Wang; lkwang@ee.nthu.edu.tw

Received 25 May 2014; Revised 9 July 2014; Accepted 14 July 2014; Published 10 August 2014

Academic Editor: Chao-Rong Chen

We demonstrate the performance improvement of p-type single-crystalline silicon (sc-Si) solar cells resulting from front surface passivation by a thin amorphous silicon (a-Si) film deposited prior to phosphorus diffusion. The conversion efficiency was improved for the sample with an a-Si film of ~5 nm thickness deposited on the front surface prior to high-temperature phosphorus diffusion, with respect to the samples with an a-Si film deposited on the front surface after phosphorus diffusion. The improvement in conversion efficiency is 0.4% absolute with respect to a-Si film passivated cells, that is, the cells with an a-Si film deposited on the front surface after phosphorus diffusion. The new technique provided a 0.5% improvement in conversion efficiency compared to the cells without a-Si passivation. Such performance improvements result from reduced surface recombination as well as lowered contact resistance, the latter of which induces a high fill factor of the solar cell.

1. Introduction

Because of long-term stability and relatively high light-to-electricity conversion, crystalline silicon (c-Si) solar cells have dominated the photovoltaic market for quite a while. Commercially, p-type silicon substrates are used as a common photovoltaic (PV) material and occupy a large majority of the PV market sales. Today, many research groups are focusing on various techniques for producing high efficiency p-type c-Si solar cells, while paying attention to the issue of cost reduction commensurate with a mass-production process. With this aim, many techniques for manufacturing silicon solar cells have been developed, including selective emitter solar cells [1–3], buried contact solar cells [4], surface passivated solar cells [5–8], back-side contact solar cells [9, 10], and heterojunction with intrinsic thin layer (HIT) solar cells [11–14].

In the PV industry, front surface passivation is quite an important technique and has been applied to improve silicon solar cells for a long time. A thermal oxide layer has been considered a good candidate material for reducing surface dangling bonds [15], while amorphous silicon nitride with hydrogen, that is, SiNx:H, has proven a good surface passivating counterpart [16, 17]. Hydrogen-rich amorphous silicon (a-Si:H), on the other hand, has been a well-known surface passivating material [5–8]. In the latter application, a-Si:H passivates the front surface of a phosphorus diffused silicon solar cell mainly owing to the annihilation of surface dangling bonds by hydrogen atoms originally residing in the a-Si:H layer. Even without hydrogen-passivation effect as stated above, a polysilicon film deposited at 620°C upon the surfaces of a phosphorus diffused silicon wafer in an LPCVD chamber proved to increase the open-circuit voltage (V_{oc}). From a lifetime test, the polysilicon film was believed to passivate the surface of the solar cell [18]. This LPCVD technique proved to improve the conversion efficiency by ~0.3% absolute with respect to conventional cells.

In this study, we present a different technique in which a thin a-Si film is deposited onto a p-type substrate prior to the phosphorus diffusion process and later turns into a

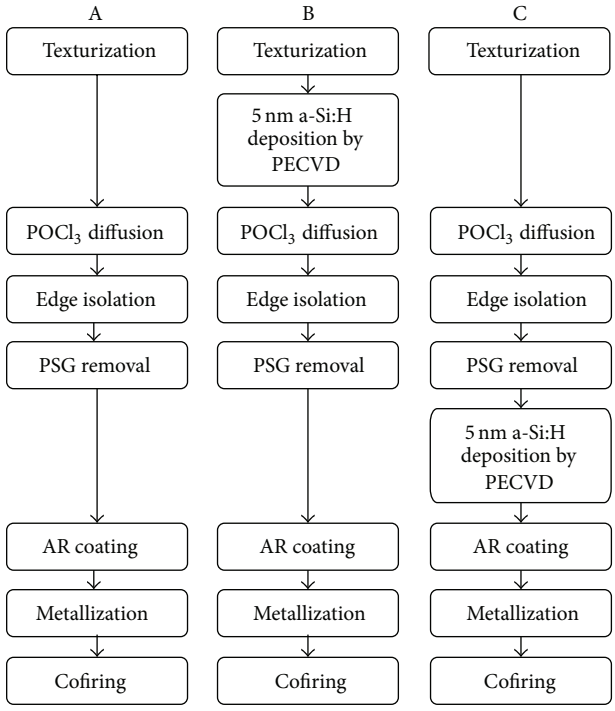

Figure 1: Process flow diagram for three groups of solar cells fabricated in this study. A, B, and C denote, respectively, the main fabrication steps for the three different groups.

polysilicon film after the phosphorus diffusion process. The polysilicon exhibits a peak dopant concentration, inducing a lower contact resistance and henceforth a higher fill factor.

In section two, three groups of solar cell samples are introduced for comparison. Group A refers to reference cells following a standard industrial production sequence and group B represents the polysilicon passivated solar cells obtained by the new technique, while group C consists of a-Si passivated solar cells with an a-Si film deposited after the phosphorus diffusion. The performances of the three groups of solar cells are compared in section three. A discussion is also given. Then section four concludes this paper.

2. Sample Preparation

We have used three groups of solar-grade p-type silicon wafers in this study for fabrication of solar cells following a standard process. The fabrication was performed mostly in a mass-production line situated at Aide Solar, a cell manufacturer in China. For all experiments in the fabrication, the silicon substrates were (100)-oriented sc-Si p-type Czochralski (Cz) wafers with resistivity in the range 1–3 Ω-cm and with an average thickness of ~190 μm. The solar wafers were pseudosquare and had a dimension of $156 \times 156\,\text{mm}^2$.

Figure 1 shows the three processes for the solar cell fabrication without showing the wafer cleaning procedures though. The wafers were divided into three groups. Group A followed fabrication steps of a standard manufacturing

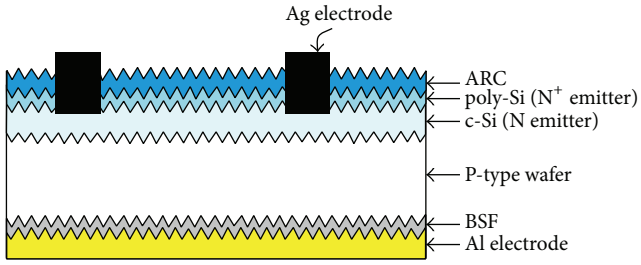

Figure 2: Cross-sectional sketch of the solar cell in group B.

process that starts with a basic cleaning, followed by texturization, $POCl_3$ diffusion, edge isolation, phosphorus glass removal, deposition of antireflection coating (ARC), metallization on both sides, and then cofiring. These procedures are described in more detail as follows. In the first step, these wafers were cleaned and then dipped in an alkaline solution with IPA additive to form a pyramid-like surface on both sides. After being cleaned and dried, the wafers were placed back to back in pair on a quartz boat and loaded into a high-temperature phosphorus diffusion furnace with $POCl_3$ as a source to form an emitter with a sheet resistance of ~ 70 Ω/square on the front side. Edge isolation was performed by plasma etching to ensure that the front-side emitter was electrically isolated from the back side. The phosphorous glass (PSG) was afterwards removed by a diluted HF solution. A SiNx film of ~82 nm thickness used as an antireflection coating (ARC) on the front surface of the cell was deposited at 450°C by plasma enhanced chemical vapor deposition (PECVD) system, followed by screen printing of aluminum paste (plus silver busbar paste) on the back surface and silver paste on the front surface in a 3-busbar H-shaped grid pattern. Finally, the two-side printed contacts were cofired in a belt furnace.

Wafers in group B followed the same process as that for group A except that the wafers were deposited to form an a-Si:H film of ~5 nm (4.8 nm, more correctly) thickness on the front surface prior to the phosphorus diffusion. The a-Si:H film was deposited by PECVD at 285°C. This step was conducted at the CNMSN (Center for Nanotechnology, Material Science and Microsystems) located at National Tsing Hua University. This step is a key requirement in optimizing the performance of solar cells in this study. Thereafter, wafers in groups B followed the steps of a standard process as stated for group A, that is, $POCl_3$ diffusion, edge isolation, deposition of ARC, metallization on both sides, and cofiring. A cross-sectional sketch of the device of this group is shown in Figure 2.

Wafers in groups C also followed the same process as that for group A except that a ~5 nm a-Si:H film was deposited on front sides of these wafers after PSG removal. Deposition of the a-Si:H films was done by PECVD at CNMSN. The difference between groups C and B resides in the order of the a-Si deposition process in the fabrication sequence. For a-Si:H passivated solar cells, process C is a common method to form surface passivation layer. Wafers in groups A were considered as a reference, while wafers in both groups of A

Table 1: Electrical characteristics of solar cell parameters measured under the standard test condition (25°C, AM 1.5 G). The average and best efficiencies obtained in the measurement are shown for each group of solar cells. Series resistances and shunt resistances for the best cell and the average are also shown.

		V_{oc} (V)	J_{sc} (mA/cm^2)	F.F. (%)	E_{ff} (%)	Rs (Ω)	Rsh (Ω)
(A) Standard cell	Average	0.623	36.19	77.55	18.01 ± 0.063	0.0056	40.23
	Best	0.625	36.26	77.70	18.07	0.0051	41.11
(B) Solar cell with poly-Si film	Average	0.630	36.46	79.15	18.51 ± 0.082	0.0038	54.13
	Best	0.631	36.57	79.24	18.61	0.0035	56.76
(C) Solar cell with a-Si film	Average	0.629	36.32	77.79	18.11 ± 0.125	0.0045	43.20
	Best	0.631	36.37	78.32	18.29	0.0041	44.65

and C were compared with group B in this study. Note that wafers of groups A and B were diffused at the same time in the same quartz boat, with almost an identical sheet resistance of 70~80 Ω/square formed. Wafers of group C were diffused earlier in the same production line, having a sheet resistance in the range of 70~80 Ω/square.

3. Results and Discussion

3.1. Conversion Efficiency Improvement. The conversion efficiencies of the solar cells were measured with a solar simulator and an IV test equipment under the standard test condition of AM 1.5 G illumination (100 mW/cm^2) at 25°C. Table 1 presents the average and best experimental data of V_{oc}, J_{sc}, and F.F. and conversion efficiency (E_{ff}) for solar cells of groups A, B, and C, respectively. There, values for the series resistance Rs and the shunt resistance Rsh are also shown. The solar cells in groups A, B, and C are, respectively, standard solar cells, the solar cells with poly-Si films, and the solar cells with a-Si films. Each group contains 15 samples. Note that the poly-Si of group-B cells was formed in the high-temperature diffusion process by crystallization of the a-Si film that was deposited prior to the diffusion and that the a-Si films of group-C cells were deposited onto the wafers after the diffusion process. On average, V_{oc} of the standard solar cells (i.e., the reference cells) is 0.623 V, J_{sc} is 36.19 mA/cm^2, and F.F. is 77.55%, and the efficiency is 18.01% (with the standard deviation δ = 0.063%). The solar cells with poly-Si films have an average efficiency of 18.51% (with δ = 0.082%) while the solar cells with a-Si films have an average efficiency of 18.11% (with δ = 0.125%). The best cell of group B has V_{oc} = 0.631 V and J_{sc} = 36.57 mA/cm^2 and a fill factor of 79.24% and an efficiency of 18.61%. Notably, this test cell has an efficiency improvement over the standard cell by 0.54% (absolute) and over the cell on group C by 0.32% (absolute).

3.2. Crystallization. In order to observe the crystallization property of silicon films deposited by PECVD followed by a high-temperature diffusion process, we deposited silicon films with a thickness of 133 nm on two quartz substrates. Then, only one of them was loaded into a high-temperature furnace at 833°C. Figure 3 shows the Raman spectra of silicon films with and without going through a high-temperature process, respectively. A broad transverse optic (TO) peak around 480 cm^{-1} in the Raman spectrum of the silicon film deposited by PECVD at 285°C without going through a high-temperature process, corresponding to amorphous silicon phase, is observed [19, 20]. The sharp TO peak around 520 cm^{-1} was obtained in the Raman spectrum of the silicon film deposited by PECVD at 285°C and subsequently going through a high-temperature process. The sharp TO peak around 520 cm^{-1} corresponds to a crystalline phase with a grain size larger than 10 nm [20, 21]. This result makes us believe that a high-temperature diffusion process rendered the original a-Si film crystallized to form a poly-Si film on the substrate. This was also confirmed by the work in high-temperature diffusion process [22].

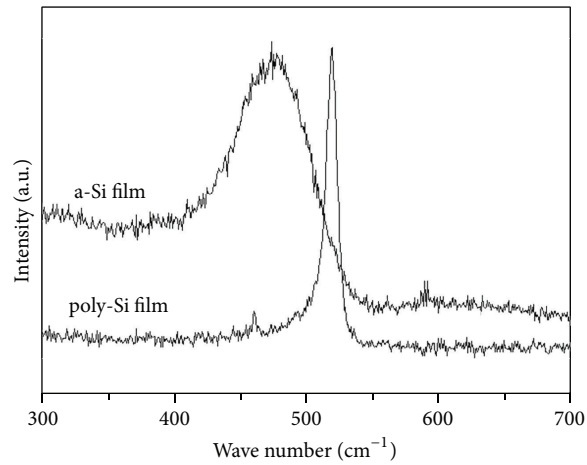

Figure 3: Raman spectra of silicon films with and without going through a high-temperature process, respectively.

In order to verify the thickness uniformity of the silicon films, we used two polished (100) sc-Si substrates and deposited silicon films with a thickness of ~5 nm on the two substrates. One of them was loaded into a high-temperature diffusion furnace with $POCl_3$ as a doping source at 833°C followed by phosphorous glass (PSG) removal. The two samples were measured by transmission electron microscopy (TEM). Figure 4 shows the TEM cross-sectional images for the films at the a-Si/sc-Si and poly-Si/sc-Si interfaces, respectively. The figure shows the thickness uniformity of both silicon films. As shown by the TEM cross-sectional images in Figure 4, the thickness of the poly-Si film formed by a high-temperature

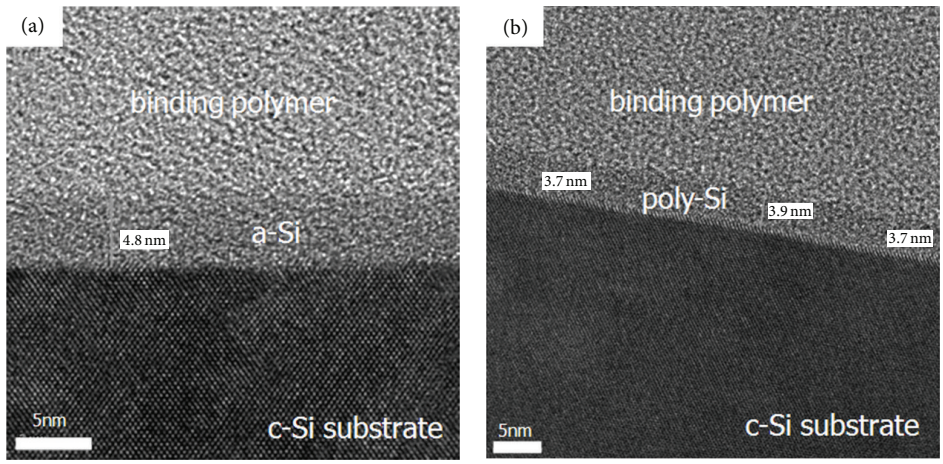

(a) (b)

FIGURE 4: Cross-sectional TEM images of (a) the a-Si film deposited by PECVD and (b) the poly-Si film formed by crystallization of a-Si after going through a high-temperature diffusion process.

diffusion process was reduced from 4.8 nm to 3.8 ± 0.1 nm owing to the PSG removal for this sample.

3.3. Open-Circuit Voltage Improvement. Open-circuit voltage is inversely related to the saturation current J_o in accordance with [23]

$$V_{\text{oc}} = \frac{kT}{q} \ln\left[1 + \frac{J_{\text{sc}}}{J_o}\right]. \quad (1)$$

Theoretically, J_o can be expressed in a simplified formula as

$$\begin{aligned} J_o &= J_{\text{ob}} + J_{\text{oe}} \\ &= \frac{qn_i^2}{N_A}\frac{D_n}{L_n} \\ &\quad \times \left[\frac{S_n \cosh\left(W_P/L_N\right) + \left(D_n/L_n\right)\sinh\left(W_P/L_N\right)}{\left(D_n/L_n\right)\cosh\left(W_P/L_N\right) + S_n \sinh\left(W_P/L_N\right)}\right] \\ &\quad + \frac{qn_i^2}{N_D}\frac{D_P}{L_P} \\ &\quad \times \left[\frac{S_P \cosh\left(W_N/L_P\right) + \left(D_P/L_P\right)\sinh\left(W_N/L_P\right)}{\left(D_P/L_P\right)\cosh\left(W_N/L_P\right) + S_n \sinh\left(W_N/L_P\right)}\right], \end{aligned} \quad (2)$$

where J_o is total saturation current density, J_{ob} and J_{oe} are the p-base and n-emitter contribution to the reverse saturation current density, (D_n, L_n) and (D_p, L_p) are the diffusivity and diffusion length of the minority carriers in the base and emitter, respectively, W_P and W_N are the base and emitter widths beyond the junction edges, and S_n and S_p are the surface recombination velocities, respectively, at the front side of the emitter and at the back side of the base [23]. Because all three groups of wafers considered here can be assumed to have the same amount of bulk defects and the same junction width, the transport behaviors of their minority carriers differ as a result of different surface conditions.

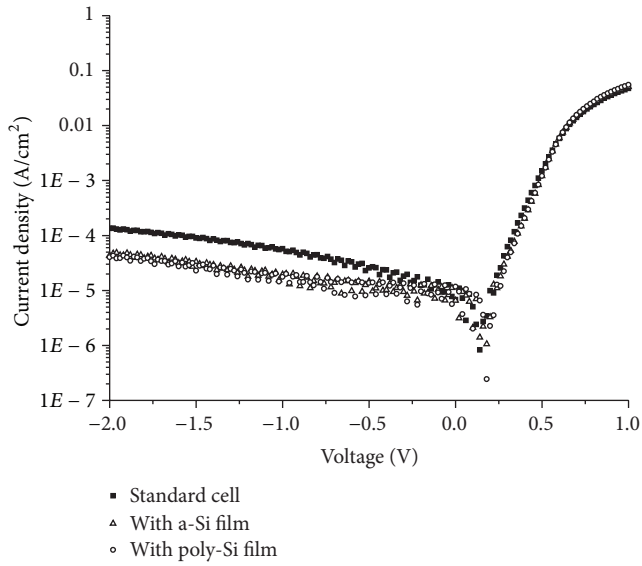

FIGURE 5: Comparison of dark log I-V plots of the standard cell (■), solar cell with an a-Si film (Δ), and solar cell with a poly-Si film (○).

From (2), a better surface passivation and henceforth a lower front surface recombination velocity S_n reduce J_o.

We measured the dark current-voltage characteristics of the three aforementioned groups of solar cells, obtaining the results in Figure 5. It can be seen that a lower saturation current density J_o is induced by surface passivation through either a-Si or poly-silicon, with respect to the case of the standard sample (i.e., the sample without silicon film deposited). This is an important evidence for the reduced surface defect density by using the a-Si or poly-Si film. Therefore, in our study we can verify that the surface recombination can be reduced by forming a poly-Si film or an a-Si film [5, 18]. It is apparent from (1) that the major benefit of reduced front surface recombination is the increase in open-circuit voltage

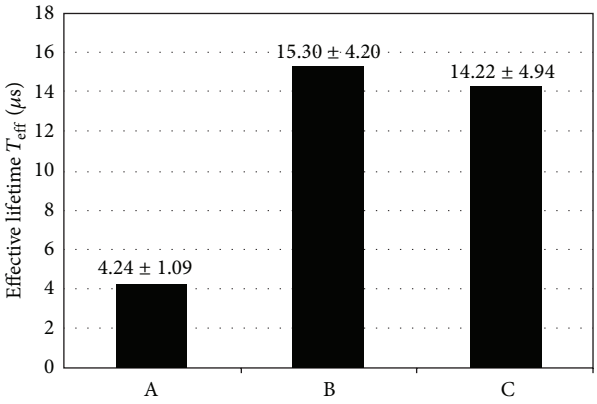

FIGURE 6: Average effective lifetimes measured for sample (A) without silicon films deposited, sample (B) with ~4 nm poly-silicon films, and sample (C) with ~5 nm a-Si films.

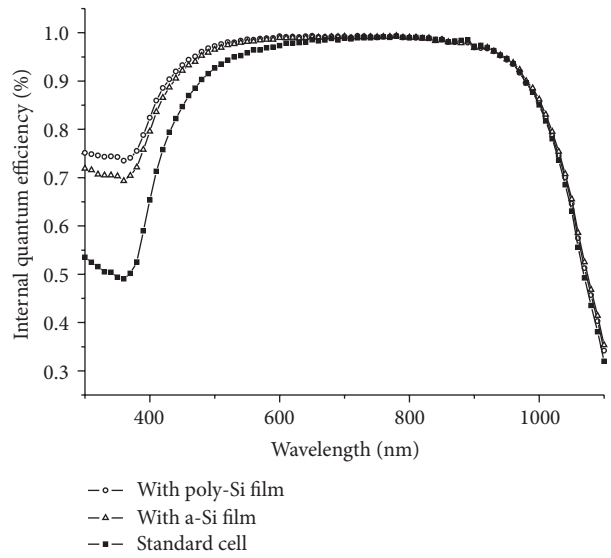

FIGURE 7: Internal quantum efficiency for a standard solar cell (-■-), a solar cell with ~4 nm poly-silicon film (-○-), and a solar cell with ~5 nm amorphous-silicon film (-Δ-).

V_{oc} which results from reduction of the saturation current J_o. This is confirmed by higher V_{oc} for cells of groups B and C than for cells of group A in Table 1.

Surface passivation effect can also be pinpointed by carrier lifetime measurement of the samples. Figure 6 shows the effective lifetimes of the samples in groups A, B, and C measured by the microwave photoconductivity decay technique (with the machine SEMILAB WT-2000). The three groups were all diffused samples without ARC deposition. Note that the samples in group A are samples without a-Si film; those in group B are samples with an about 4 nm poly-Si film and those in group C are samples with an about 5 nm a-Si film. An average effective lifetime was obtained from 16-point data measured for each sample, with each group including 15 samples. The effective lifetimes were 4.24, 15.30, and 14.22 μs, respectively, for groups A, B, and C. The standard deviations for the three groups A, B, and C were, respectively, 1.09, 4.20, and 4.94 μs. According to the Shockley-Read-Hall theory, the surface recombination rate is proportional to the density of the surface states. Because the bulk lifetimes of these samples used in the study were about the same, the increase in effective lifetime as measured was attributed to a reduction in surface recombination velocity [24].

In this study, we used silicon films with a ~5 nm thickness for surface passivation. The thickness of silicon films needs to be limited to avoid absorption of light by the silicon film in the UV-blue range [25, 26]. We believe that the a-Si and poly-Si films with a ~5 nm thickness are beneficial to the conversion efficiency for the following additional reasons. First, a thinner silicon film avoids the hindrance of electron transport which results from unsaturated bonds, grain boundaries, and other defects which act as recombination centers. Secondly, hydrogen atoms in the silicon nitride AR coating can more easily move across a thinner silicon film toward the Si film/c-Si interface and accordingly passivate the interfacial defects.

To further clarify the passivation effect, the internal quantum efficiency (IQE) was measured and shown in Figure 7 as a function of the optical wavelength ranging from 300 to 1100 nm for the three groups of solar cells. The spectral responses for the three groups of solar cells are an indication of surface passivation by a-Si and poly-Si films. As shown, there is a major difference in IQE at wavelengths of 300~600 nm between the film passivated cells and the standard cells, indicating an improvement in short-wavelength IQE by the poly-Si film with respect to the standard cells. Passivation by a-Si film can be also observed at the shorter wavelengths. And this has been reflected by the dark I-V characteristics shown in Figure 5 as well as the lifetime data shown in Figure 6. In summary, the surface passivation by both silicon films results in an improved performance in IQE as well as in open-circuit voltage.

3.4. Fill Factor Improvement. The diffusion profiles in the emitters of the standard cell, the cell with ~5 nm amorphous-silicon film, and the cell with ~4 nm poly-silicon film were analyzed by spreading resistance profile (SRP) technique. These samples were diffused in the same diffusion furnace. Figure 8 indicates that junction depths of all the cell samples were around 0.4 μm. The sample with a-Si film and the standard solar cell sample have an identical phosphorus concentration profile because the a-Si film was deposited on the as-diffused sample (see the dotted and the dashed curves). However, there exists a narrow peak on the concentration profile of the poly-Si film deposited sample. Such a peak was formed by the low activation energy of the phosphorus impurities in a-Si. This can be explained as follows. Diffusion of phosphorus at a high temperature in a-Si was carried out by migration through a large number of vacancies in a-Si in a high-temperature environment [27]. The activation energy of the phosphorus diffusion in a-Si is lower than that in sc-Si. Thus, in the process of $POCl_3$ diffusion after a-Si deposition, more phosphorus atoms diffuse into the a-Si film than into the sc-Si substrate, leading to a higher phosphorus

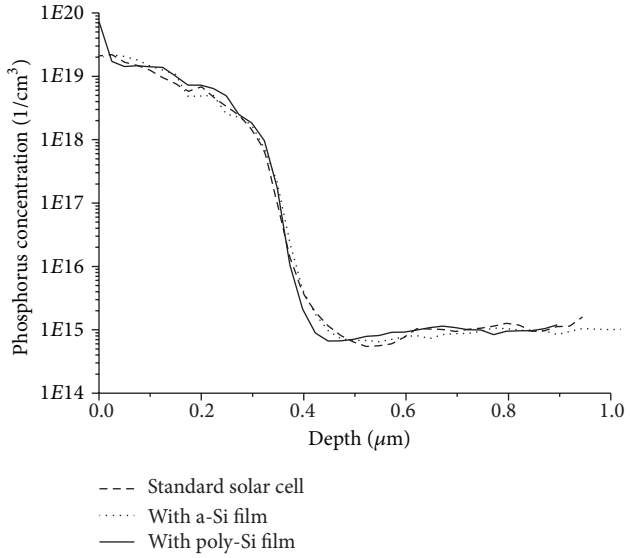

FIGURE 8: Spreading resistance profiles of phosphorus concentration in the emitter of a standard cell (- - -), a cell with ~5 nm amorphous-silicon film (···), and a cell with ~4 nm poly-silicon film (—).

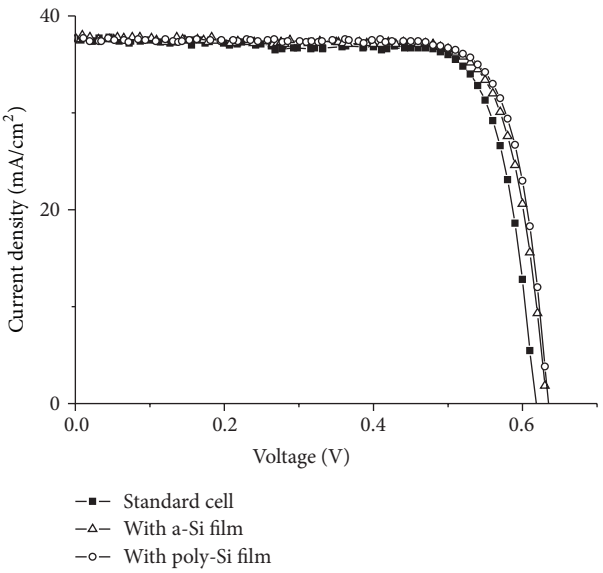

FIGURE 9: *I-V* plots of a standard cell (■), a cell with poly-Si film (○), and a cell with a-Si film (Δ) obtained under the standard test condition.

concentration in the a-Si film (which was later transformed into a poly-Si film during the high-temperature process) than in the sc-Si region. The high phosphorus concentration in the poly-silicon film forms a low-contact resistance and therefore enhances the fill factor.

Figure 9 shows the measured *I-V* curves for the three different solar cells under the standard test condition. Obviously, the solar cells with a poly-silicon film and with an a-Si film outperform the standard solar cell. It appears that surface passivation by poly-silicon film and a-Si film reduces the surface defects and thus improves V_{oc}. The solar cells with polysilicon film presented the best efficiency among the three different solar cells. It is not only because the reduced surface recombination in solar cell with a polysilicon film improves V_{oc}, but also because the low-contact resistance improves the FF. The latter is evident from the data shown in Table 1.

It should be noted that the ARC (which is a silicon nitride film) is supposed to be a passivation layer as well. However, the ARC was deposited at the temperature of 450°C, making a large part of hydrogen atoms diffuse out and henceforth weakening the passivation effect. To date, some cell manufacturers have lowered the ARC deposition temperature to 400°C with a view to enhancing the passivation effect. The passivation effect resulting from the hydrogen atoms that reside in the ARC and are supposed to fix the dangling bonds at the surface of the silicon wafer is still limited. We have measured the lifetimes of diffused wafers with and without an ARC and found that the increase in lifetime with an ARC is only incremental. Therefore, it may be considered that the passivation results mostly from the thin silicon film, especially the poly-Si film.

The a-Si:H film deposited after phosphorous diffusion contributes many hydrogen atoms for fixing the dangling bonds and thereof upgrades the lifetime, as indicated in Figure 6 for the case without ARC. On the other hand, the poly-Si film for the case of group B cells is found to improve the lifetime without the hydrogen atoms for passivation. However, such passivation is believed to come from the heavily doped poly-Si layer as mentioned in Section 3.4. The heavy doping in such a layer induces a strong field, rejecting photogenerated holes and henceforth reducing the electron/hole recombination at the surface. And because the poly-Si film is so thin that there is not much photogenerated carriers in there, optical response at short wavelengths is not weakened. It is noted that the passivation from a-Si film for the case of group C cells remains at the ARC deposition temperature, 450°C, although the a-Si loses some of its hydrogen atoms at such a temperature.

4. Conclusions

We have presented a new approach to increase the open-circuit voltage (V_{oc}), the fill-factor (FF), and henceforth the conversion efficiencies of the solar cells by depositing an a-Si film prior to the standard diffusion process. The conversion efficiency was improved by 0.5% absolute with respect to the standard solar cell, in the case that the $POCl_3$ diffusion process was treated after the deposition of a-Si film on the front side of a solar cell. The improvement in conversion efficiency was 0.4% absolute with respect to the cells with a-Si deposition after the $POCl_3$ diffusion process. Raman spectra of the silicon film with a high-temperature diffusion process indicate that an a-Si film became a poly-Si film. Dark *I-V* characteristics and the effective lifetimes of three groups of samples (i.e., standard solar cells, the solar cells with a-Si films, and the solar cells with poly-silicon films) demonstrate the surface passivation effect induced by the poly-silicon film on the surface of solar cell. The measurements indicate that the decrease of surface defect density and the reduction of

recombination rate can be achieved by a poly-silicon film. The spectral responses of internal quantum efficiency in the short wavelength range also shows the improvement due to reduced surface recombination rates on the front surface of the cell. Spreading resistance profile of the poly-Si deposited solar cells can explain the increase in the fill factor of the solar cell. Therefore, the high-temperature $POCl_3$ diffusion process after the deposition of an a-Si film on the front sides of a silicon solar cell proves to be an effective means in obtaining performance-improved silicon solar cells.

Conflict of Interests

The authors declare that there is no conflict of interests regarding the publication of this paper.

Acknowledgments

The authors would like to thank the Jiangsu Aide Solar, Energy Tech. Co., Ltd., Xuzhou, China, National Tsing Hua University, Hsinchu, Taiwan, and the Grant 103-3113-E-007-003 from MOST, Taiwan, for financially supporting this research.

References

[1] A. Dastgheib-Shirazi, H. Haverkamp, B. Raabe, F. Book, and G. Hahn, "Selective emitter for industrial solar cell production: a wet chemical approach using a single side diffusion process," in *Proceedings of the 23rd European Photovoltaic Solar Energy Conference and Exhibition (Euro-PVSEC '08)*, pp. 1197–1199, 2008.

[2] F. Book, B. Raabe, and G. Hahn, "Two diffusion step selective emitter: comparison of mask opening by laser or etching paste," in *Proceedings of the 23rd Euro-PVSEC*, pp. 1546–1549, 2008.

[3] R. Monna, N. Enjalbert, Y. Veschetti, M. Lozac'h, and M. Pirot, "17.8% efficiency obtained on c-Si solar cells using a selective emitter industrial type process," in *Proceedings of the 23rd European Photovoltaic Solar Energy Conference and Exhibition (Euro-PVSEC '08)*, pp. 1733–1736, 2008.

[4] S. R. Wenham, C. B. Honsberg, S. Edmiston et al., "Simplified buried contact solar cell process," in *Proceedings of the 1996 25th IEEE Photovoltaic Specialists Conference*, pp. 389–392, May 1996.

[5] S. Olibet, E. Vallat-Sauvain, and C. Ballif, "Model for a-Si:H/c-Si interface recombination based on the amphoteric nature of silicon dangling bonds," *Physical Review B*, vol. 76, no. 3, Article ID 035326, 2007.

[6] S. de Wolf, S. Olibet, and C. Ballif, "Stretched-exponential a-Si:Hc-Si interface recombination decay," *Applied Physics Letters*, vol. 93, no. 3, Article ID 032101, 2008.

[7] T. F. Schulze, H. N. Beushausen, C. Leendertz, A. Dobrich, B. Rech, and L. Korte, "Interplay of amorphous silicon disorder and hydrogen content with interface defects in amorphous/crystalline silicon heterojunctions," *Applied Physics Letters*, vol. 96, no. 25, Article ID 252102, 2010.

[8] J. Damon-Lacoste, L. Fesquet, S. Olibet, and C. Ballif, "Ultra-high quality surface passivation of crystalline silicon wafers in large area parallel plate reactor at 40 MHz," *Thin Solid Films*, vol. 517, no. 23, pp. 6401–6404, 2009.

[9] E. Schneiderlöchner, R. Preu, R. Ldemann, and S. W. Glunz, "Laser-fired rear contacts for crystalline silicon solar cells," *Research and Applications*, vol. 10, no. 1, pp. 29–34, 2002.

[10] R. Woehl, J. Krause, F. Granek, and D. Biro, "19.7% efficient all-screen-printed back-contact back-junction silicon solar cell with aluminum-alloyed emitter," *IEEE Electron Device Letters*, vol. 32, no. 3, pp. 345–347, 2011.

[11] M. Tanaka, S. Okamoto, S. Tsuge, and S. Kiyama, "Development of HIT solar cells with more than 21% conversion efficiency and commercialization of highest performance HIT modules," in *Proceddings of the 3rd World Conference on Photovoltaic Energy Conversion*, vol. 1, pp. 955–958, May 2003.

[12] E. Maruyama, A. Terakawa, M. Taguchi et al., "Sanyo's challenges to the development of high-efficiency HIT solar cells and the expansion of HIT business," in *Proceedings of the IEEE 4th World Conference on Photovoltaic Energy Conversion (WCPEC '06)*, pp. 1455–1460, May 2006.

[13] L. Zhao, H. L. Li, C. L. Zhou, H. W. Diao, and W. J. Wang, "Optimized resistivity of p-type Si substrate for HIT solar cell with Al back surface field by computer simulation," *Solar Energy*, vol. 83, no. 6, pp. 812–816, 2009.

[14] V. A. Dao, J. Heo, H. Choi et al., "Simulation and study of the influence of the buffer intrinsic layer, back-surface field, densities of interface defects, resistivity of p-type silicon substrate and transparent conductive oxide on heterojunction with intrinsic thin-layer (HIT) solar cell," *Solar Energy*, vol. 84, no. 5, pp. 777–783, 2010.

[15] A. W. Stephens, A. G. Aberle, and M. A. Green, "Surface recombination velocity measurements at the silicon-silicon dioxide interface by microwave-detected photoconductance decay," *Journal of Applied Physics*, vol. 76, no. 1, pp. 363–370, 1994.

[16] M. J. Kerr and A. Cuevas, "Very low bulk and surface recombination in oxidized silicon wafers," *Semiconductor Science and Technology*, vol. 17, no. 1, pp. 35–38, 2002.

[17] H. F. W. Dekkers, S. de Wolf, G. Agostinelli, F. Duerinckx, and G. Beaucarne, "Requirements of PECVD SiN_x:H layers for bulk passivation of mc-Si," *Solar Energy Materials and Solar Cells*, vol. 90, no. 18-19, pp. 3244–3250, 2006.

[18] C. T. Li, F. C. Hsieh, and L. K. Wang, "Performance improvement of p-type silicon solar cells with thin silicon films deposited by low pressure chemical vapor deposition method," *Solar Energy*, vol. 88, pp. 104–109, 2013.

[19] M. Z. Lai, P. S. Lee, and A. Agarwal, "Thermal effects on LPCVD amorphous silicon," *Thin Solid Films*, vol. 504, no. 1-2, pp. 145–148, 2006.

[20] D. Beeman, R. Tsu, and M. F. Thorpe, "Structural information from the Raman spectrum of amorphous silicon," *Physical Review B*, vol. 32, no. 2, pp. 874–878, 1985.

[21] S. Y. Lien, B. R. Wu, J. C. Liu, and D. S. Wuu, "Fabrication and characteristics of n-Si/c-Si/p-Si heterojunction solar cells using hot-wire CVD," *Thin Solid Films*, vol. 516, no. 5, pp. 747–750, 2008.

[22] H. Kim, J. Choi, and J. Lee, "Effects of silicon-hydrogen bond characteristics on the crystallization of hydrogenated amorphous silicon films prepared by plasma enhanced chemical vapor deposition," *Journal of Vacuum Science and Technology A*, vol. 17, no. 6, pp. 3240–3245, 1999.

[23] A. Rohatgi and P. Rai-Choudhury, "Design, fabrication, and analysis of 17-18-percent efficient surface-passivated silicon solar cells," *IEEE Transactions on Electron Devices*, vol. 31, no. 5, pp. 576–601, 1984.

[24] T. Mueller, S. Schwertheim, M. Scherff, and W. R. Fahrner, "High quality passivation for heterojunction solar cells by hydrogenated amorphous silicon suboxide films," *Applied Physics Letters*, vol. 92, no. 3, Article ID 033504, 2008.

[25] P. P. Altermatt, H. Plagwitz, R. Bock et al., "The surface recombination velocity at boron-doped emitters comparison between various passivation techniques," in *Proceedings of the 21st European Photovoltaic Solar Energy Conference*, pp. 647–650, 2006.

[26] H. Fujiwara and M. Kondo, "Effects of a-Si:H layer thicknesses on the performance of a-Si:H/c-Si heterojunction solar cells," *Journal of Applied Physics*, vol. 101, no. 5, Article ID 054516, 2007.

[27] A. F. Khokhlov, V. A. Panteleev, E. V. Dobrokhotov, G. A. Maksimov, and V. A. Sidorov, "Phosphorus Diffusion in Amorphous Silicon," *Physica Status Solidi (A) Applied Research*, vol. 81, no. 1, pp. K15–K18, 1984.